

Cite this article as: Xing Tong, Liu Cuirong, Ma Lifeng, et al. Neutral Layer Offset Rule in Straightening Process of S304/Q235 Composite Plate with Different Thickness Ratios[J]. Rare Metal Materials and Engineering, 2022, 51(11): 4085-4092.

ARTICLE

Neutral Layer Offset Rule in Straightening Process of S304/Q235 Composite Plate with Different Thickness Ratios

Xing Tong^{1,2}, Liu Cuirong³, Ma Lifeng¹, Li Qiang⁴, Li Yugui², Chu Zhibing^{1,3}, Wang Xiaogang¹, Gui Hailian^{1,3}

¹ Engineering Research Center of Heavy Mechanical, Ministry of Education, Taiyuan University of Science and Technology, Taiyuan 030024, China; ² School of Mechanical Engineering, Taiyuan University of Science and Technology, Taiyuan 030024, China; ³ School of Material Science and Engineering, Taiyuan University of Science and Technology, Taiyuan 030024, China; ⁴ Technology Center, Taiyuan Heavy Industry Co., Ltd, Taiyuan 030024, China

Abstract: To improve the accuracy of the straightening process of S304/Q235 composites, the elastic-plastic deformation and straightening process of the bimetal composite plates were investigated by the Abaqus finite element software. In addition, the neutral layer offset of the bimetal composite plates with different thickness ratios was also analyzed. Results show that the neutral layer offset is dependent on the yield strength and thickness ratio of composite plates. The theoretical calculations, numerical simulations, and experiment results are compared. Then the fitting formula for neutral layer offset is obtained and verified. Additionally, the dynamic change of the neutral layer offset state was analyzed. This research provides the theoretical basis for the establishment of high precision straightening force model.

Key words: thickness ratio; neutral layer offset; bimetal composite plate; straightening

The bimetal composite plates have been widely used in the traditional and high-tech industries, owing to their low cost and excellent composite performance^[1-4]. However, during the manufacturing process of bimetal composite plates, the shape defects, such as waving, ladle bending, and sickle bending, usually appear^[5]. Generally, these defects are caused by the external environment factors and material differences in the bonding layer of bimetal composite plates, which should be considered in the subsequent processing and application of bimetal composite plates^[6,7]. Therefore, the shape defects of bimetal composite plates should be eliminated as much as possible^[8,9].

The straightening of bimetal composite plates is an essential manufacture process^[10,11]. Recently, the properties of bimetal composite plates after straightening have been widely researched^[12-14]. Morris et al^[15] described the influence factors for the straightening process of metal plates with the five-roll

straighteners and found that the straightening is affected by the wrap angle and yield stress. Huh et al^[16] analyzed the straightening process of strips by the finite element method, and investigated the maximum stress strain and residual stress under the steady state. Kano et al^[17] explored the deformation of workpieces in the straightener through the elastic-plastic finite element method, and discussed the influence of the Bauschinger effect on the residual stress after straightening. Meanwhile, the isotropic strengthening material model and the kinematic strengthening model have been compared. Cui et al^[18] distinguished the residual stress by the curvature integral method. Guan^[19] and Zhang^[20] et al analyzed the section bending characteristics of bimetal composite plates during the straightening process by the curvature integral method. It is found that the neutral layer of the steel/aluminum composite plates appears during the straightening process. Dharani et al^[21] investigated the bending stress, deflection, and

Received date: December 08, 2021

Foundation item: National Key Research and Development Project (2018YFA0707305, 2018YFB1307902); Major Special Projects of Science and Technology in Shanxi Province (20181102016); National Natural Science Foundation of China (51675362); Sponsored by Shanxi Scholarship Council of China (2017-081); Key Projects of Shanxi Key R&D Program (201703D111003); Shanxi Graduate Innovation Project (2021Y674)

Corresponding author: Gui Hailian, Ph. D., Professor, School of Material Science and Engineering, Taiyuan University of Science and Technology, Taiyuan 030024, P. R. China, E-mail: guihailian@tyust.edu.cn

Copyright © 2022, Northwest Institute for Nonferrous Metal Research. Published by Science Press. All rights reserved.

neutral layer of thin cylindrical and rectangular composite plates, and determined that the composite materials have different transverse shear moduli and elastic properties. Moreover, the specific values of those properties can be determined by applying tension and compression along the fiber direction. Wang^[22] and Huang^[23] et al proved that the neutral layer offset coefficient is directly proportional to the internal grain size of magnesium alloy. It is also proved that the neutral layer offset is gradually increased with increasing the grain size during the V-bending tests. Combining the tension and bending experiments, the bar straightening model has also been studied^[24]. It is concluded that the neutral layer offset is related to the reverse bending radius, mechanical properties, bar specifications, initial degree of bending, and the straightening forces. When the maximum reverse bending deflection is greater than 15 mm, the neutral layer offset should be taken into consideration. Besides, the position of the neutral layer changes greatly during the bending process, and the neutral layer is gradually transferred to the thin plate when the bending radius of the die is decreased^[25]. Zhao et al^[26] studied the phenomenon of neutral layer offset in the bending process of a box structure. The formulae for the neutral layer with the symmetrical and asymmetrical box structures are obtained, and the error between the theoretical and experimental results is less than 5%.

The neutral layer offset of bimetal composites during the straightening process has been analyzed by the boundary finite element method and elastic-plastic method^[27-31]. The neutral layer offset formula was deduced and verified. In addition, the bending moment and straightening force during straightening process were obtained according to the neutral layer offset theory. The obtained formula was verified by the finite element method and compared with the experiment data. Furthermore, the effect of neutral layer offset on the straightening process of composites was discussed.

The straightening accuracy can influence the properties of the bimetal composite plates. The formula of the neutral layer was deduced via the stress and strain during the bending process, and the influence factors of the neutral layer offset were discussed. Moreover, the relationship between the thickness ratio and the neutral layer of bimetal composite plates was explored by the finite element method. In addition, the stress state of composite plates was analyzed during the simulation process. This research provides guidance for the optimization of the straightening process, leading to the quality assurance for subsequent processing.

1 Neutral Layer Offset Theory of Bimetal Composite Plates

With the ideal elastic-plastic material which obeys the Hooke's law in the elastic stage, the stress neutral layer offset of composite plates during the bending process was analyzed. The linear change can be observed in the plastic stage after the surface equivalent stress reaches the yield strength. Since the

straightening process includes the continuous bending with multi-roll pressing, the plates undergo a complex elastic-plastic process. The conditions of the elastic-plastic change during the straightening process are different when the plates pass through different straightening rolls. The straightening process can be divided into three stages. The first stage is the straightening process of pressing reduction when the straightener enters, and the elastic-plastic deformation of both layers occurs in this stage. The second stage is the elastic deformation of the basic layer when the straightener is at the smooth straightening stage. The third stage is the adjustment stage, in which both layers are at the elastic stage. The stress states of different stages are shown in Fig.1~Fig.3. The stress state of the single-layer material plate during the straightening is shown in Fig.4.

In Fig.1 and Fig.2, h_c is the thickness of the clad layer; e_c is the neutral layer offset of the clad layer; σ_{c1} is the surface stress of the clad layer; σ_{c2} is the interface stress of the clad layer; z_{c1} is the upper elastic thickness of the clad layer and z_{c2} is the lower elastic thickness of the clad layer; h_b is the thickness of the base layer; e_b is the neutral layer offset of the base layer; σ_{b1} is the interface stress of the base layer; σ_{b2} is the surface stress of the base layer; z_{b1} is the upper elastic thickness of the base layer; z_{b2} is the lower elastic thickness of the base layer.

In Fig.3, σ_c is the surface stress of the clad layer and σ_b is the interface stress of the base layer.

In Fig.4, $2h$ is the thickness of single-layer plate, e is the neutral layer offset of single-layer plate, σ_{y1} is the upper surface stress of single-layer plate, σ_{y2} is the lower surface stress of single-layer plate, y_1 is the upper elastic thickness of single-layer plate, and y_2 is the lower elastic thickness of single-layer plate.

As shown in Fig.4, it can be seen that the upper part of the plate is subjected to the straightening force along the negative

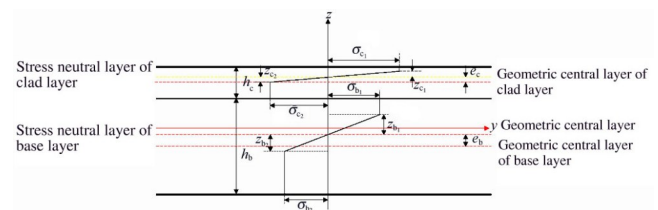


Fig.1 Stress states of clad layer and base layer during elastic-plastic deformation at the first stage

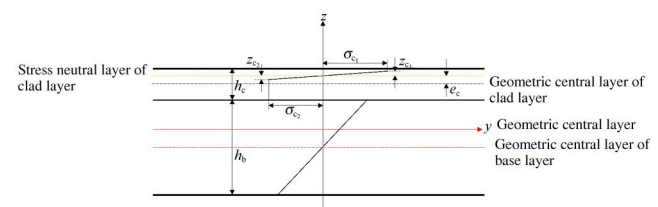


Fig.2 Stress states of clad layer during elastic-plastic deformation and base layer during elastic deformation at the second stage

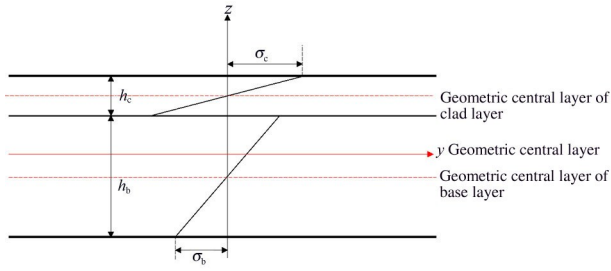


Fig.3 Stress states of clad layer and base layer during elastic deformation at the third stage

z-axis, and line BC represents the central axis of the plate.

$$\sigma_s = \frac{1}{\sqrt{2}} \sqrt{(\sigma_x - \sigma_y)^2 + (\sigma_x - \sigma_z)^2 + (\sigma_y - \sigma_z)^2 + 6(\tau_{xy}^2 + \tau_{xz}^2 + \tau_{yz}^2)} = \sqrt{3} k \quad (1)$$

where $\sigma_x, \sigma_y, \sigma_z, \tau_{xy}, \tau_{xz},$ and τ_{yz} are the six-dimensional stress components; k is the shear yield strength.

Because the equivalent stress formula of Mises plastic deformation is derived from the principal stress, the equation can be transformed into Eq.(2), as follows:

$$\sigma_s = \frac{1}{\sqrt{2}} \sqrt{(\sigma_1 - \sigma_2)^2 + (\sigma_1 - \sigma_3)^2 + (\sigma_2 - \sigma_3)^2} = \sqrt{3} k \quad (2)$$

where $\sigma_1, \sigma_2,$ and σ_3 are the main stresses. For the general plane strain, $\sigma_1 > \sigma_2 > \sigma_3$ is adopted. According to the incremental theory, Eq.(3) can be obtained, as follows:

$$\sigma_2 = \sigma_m = \frac{1}{2}(\sigma_1 + \sigma_3) \quad (3)$$

where σ_m is the mean stress.

By substituting Eq.(3) into Eq.(2), Eq.(4) can be obtained, as follows:

$$\sigma_1 - \sigma_3 = \frac{2}{\sqrt{3}} \sigma_s \quad (4)$$

According to Fig.4, the stress state at point B on the upper surface of the single-layer material is $\sigma_y = \sigma_{y1}, \sigma_z = 0,$ and $\tau_{yz} = 0.$ According to the incremental theory, $\tau_{xy} = \tau_{xz} = \tau_{yz}.$ σ_{s1} is the yield strength of clad layer; σ_{s2} is the yield strength of base layer. Therefore, the main stress at point B is $\sigma_1 = \sigma_{y1}, \sigma_3 = 0, \sigma_2 = \frac{1}{2}(\sigma_1 + \sigma_3) = \frac{1}{2}\sigma_{y1},$ and $\sigma_{s1} = \frac{\sqrt{3}}{2}\sigma_{y1}.$ The main stress at point C is $\sigma_1 = \sigma_{y2}, \sigma_3 = 0, \sigma_2 = \frac{1}{2}(\sigma_1 + \sigma_3) = \frac{1}{2}\sigma_{y2},$ and $\sigma_{s2} = \frac{\sqrt{3}}{2}\sigma_{y2}.$

It is assumed that e is the stress neutral layer offset of the ideal elastic-plastic material during bending deformation, and $2h$ is the plate thickness. Therefore, as shown in Fig.4, along the central axis BC, because the total force along z-axis $\sum F_z = 0,$ Eq.(5) can be obtained, as follows:

$$\sigma_{y1}(h - y_1 - e) + \frac{1}{2}\sigma_{y1}y_1 = \sigma_{y2}(h - y_1 + e) + \frac{1}{2}\sigma_{y2}y_2 \quad (5)$$

Since the middle elastic region conforms to Hooke's law, the variation is linear, and Eq.(6) can be obtained, as follows:

$$n = \frac{\sigma_{s1}}{\sigma_{s2}} = \frac{y_1}{y_2} \quad (6)$$

where n is the scale factor.

Because $\sigma_{s1} = \frac{\sqrt{3}}{2}\sigma_{y1}$ and $\sigma_{s2} = \frac{\sqrt{3}}{2}\sigma_{y2},$ Eq. (6) can be

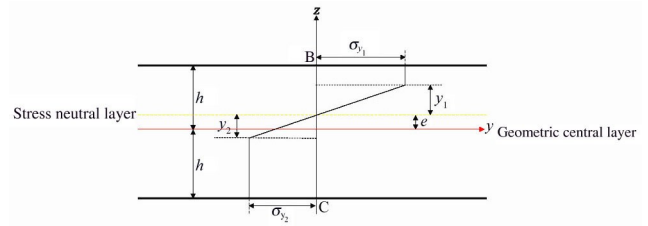


Fig.4 Stress state of single-layer material plate during elastic-plastic deformation

The equivalent stress formula of Mises plastic forming is as follows:

transformed into Eq.(7), as follows:

$$n = \frac{\sigma_{s1}}{\sigma_{s2}} = \frac{y_1}{y_2} = \frac{\sigma_{y1}}{\sigma_{y2}} \quad (7)$$

By substituting Eq.(7) into Eq.(5), Eq.(8) can be obtained, as follows:

$$e = \frac{n-1}{n+1}h + \frac{1}{2}(1-n)y_2 \quad (8)$$

Therefore, the neutral layer offset of the single-layer material during the straightening process can be calculated. Similarly, the neutral layer offset of composite plate materials during the straightening process can also be obtained.

As shown in Fig.1, the elastic-plastic deformation occurs in both the clad layer and base layer of the composite plate. Thus, in the composite material, the stress neutral layer offset of the clad layer and base layer can be calculated by Eq.(9) and Eq.(10), respectively:

$$e_c = \frac{1}{2} \frac{n_c - 1}{n_c + 1} h_c + \frac{1}{2} (1 - n_c) z_{c2} \quad (9)$$

$$e_b = \frac{1}{2} \frac{n_b - 1}{n_b + 1} h_b + \frac{1}{2} (1 - n_b) z_{b2} \quad (10)$$

where e is the stress neutral layer offset; n_c is the scale factor of clad layer; n_b is the scale factor of base layer; the subscripts c and b represent the clad layer and base layer, respectively. Therefore, the stress neutral layer offset of the composite plate is as follows:

$$e = \alpha_1 e_c + \alpha_2 e_b \quad (11)$$

where α_1 and α_2 are weighted coefficients of the neutral layer offset, which are related to the thickness and yield strength of the material. When the thickness of base layer is much larger than that of the clad layer ($h_b \ll h_c$), or the yield strength of the base layer is much larger than that of the clad layer ($\sigma_{s2} \gg \sigma_{s1}$), the neutral layer offset of the composite plate is approximately $e_b.$

As shown in Fig.2, the elastic-plastic deformation occurs in the clad layer, and only the elastic deformation occurs in the base layer. Thus, the stress neutral layer becomes the geometric center layer, and the neutral layer offset becomes 0. In the clad layer, the stress neutral layer offset is as follows:

$$e_c = \frac{1}{2} \times \frac{n-1}{n+1} h_c + \frac{1}{2} (1-n) z_{c2} \quad (12)$$

Therefore, the stress neutral layer offset of the composite plate is as follows:

$$e = e_c = \frac{1}{2} \times \frac{n-1}{n+1} h_c + \frac{1}{2} (1-n) z_c \quad (13)$$

As shown in Fig.3, the stress neutral layer of the clad layer is located at $\frac{1}{2} h_c$, the stress neutral layer of the base layer is located at $\frac{1}{2} h_b$, and the geometric center layer of the composite plate is located at $\frac{1}{2} (h_c + h_b)$. Therefore, the stress neutral layer offset of the composite plate does not occur during the third stage.

2 Finite Element Simulation of Neutral Layer Offset in Composite Plates

Through the Abaqus finite element software, the straightening process model of bimetal composite plates was established, as shown in Fig.5. The straightening temperature was 450 °C, and the original curvature of the composite plate was 0. The full hydraulic screwdown system straightener was used as a prototype, so the degree of bending in the straightening process could be accurately adjusted. The basic parameters of the straightener are shown in Table 1, and the specific values of the bending amount are shown in Table 2. During the strengthening process, the fixed roll can prevent the warping of plate tail. The movement of the working roll was restricted in three directions, and the rotation along the x and y axes was constrained.

For the composite plate, the base layer material was Q235 steel and the clad layer material was S304 stainless steel. The length of composite plate was 900 mm, the width was 50 mm, and the total thickness was 6 mm. The basic parameters of the composite plate are shown in Table 3. The thickness ratio of the clad layer to base layer was 1:1, 1:3, and 1:5. The isotropic elastic-plastic material model was used, and the work hardening modulus was $0.01E$ (E is the elastic modulus)^[32]. The mesh of the composite plate was divided by the C3D8R division format with the eight nodes linear hexahedron element, reduced integral, and hourglass control. Each mesh unit was 5 mm×5 mm×0.5 mm, and 19 200 units were used.

To analyze the elastic-plastic deformation of the composite plate during the straightening process, 8 elements (A~H) were

selected from the grid division of the composite plate, as shown in Fig.6. Elements A~D are at the half length area of the plate, and elements E~H are the at the half width area of the plate. Meanwhile, elements A and E are at the upper surface of the composite plate; elements B and F are at the bonding layer of the clad layer; elements C and G are at the bonding layer of the base layer; elements D and H are at the lower surface of the composite plate.

The equivalent Mises stresses at elements A~H of bimetal composite plate in the straightening process are shown in Fig. 7. It can be seen that there are five extremum values of equivalent Mises stress in the composite plate, which occur when the composite plate is in contact with the upper roller during the straightening process. The maximum equivalent Mises stress is obtained at the 6# roll. The equivalent Mises stress on the lower surface of the composite plate is slightly greater than that on the upper surface, which is related to the straightening force and bending moment of the straightening roll.

According to Fig.7a and 7b, the equivalent Mises stress on both width-sides of composite plate during the straightening process is basically the same as that on the length-sides. This is because the width of the straightening roll is longer than that of the composite plate, leading to the more uniform straightening force on the composite plate along y -axis direction. However, the residual stress is different with different thickness ratios after the straightening process. Moreover, elements B, C, F, and G are at the bonding layers of the composite plate. As shown in Fig. 7, the equivalent Mises stress of the bonding layer is increased with decreasing the proportion of clad layer thickness, and it is close to the equivalent Mises stress on the composite plate surface. By comparing elements B and C, it can be seen that the equivalent Mises stress of the upper layer is greater than that of the lower layer due to the difference in yield strength of different materials.

The equivalent plastic strains of elements A~H during the straightening process are shown in Fig.8. It can be seen that the equivalent plastic strain of the clad layer surface is less than that of the base layer surface throughout the whole straightening process. The equivalent plastic strain of the bonding layer close to the clad layer surface is always less than that close to the base layer surface. It is also known that the selected elements do not enter the straightening roll, so the equivalent effect becomes zero between 0.00~8.64 s. Afterwards, the equivalent plastic strain gradually increases, which is affected by the straightening roll. The equivalent plastic strains of elements A~G are increased rapidly due to the downward reverse bending force when the composite plate passes from the 2# roll to the 4# roll between 8.16~9.60 s. Since the Bauschinger effect can reduce the yield strength of

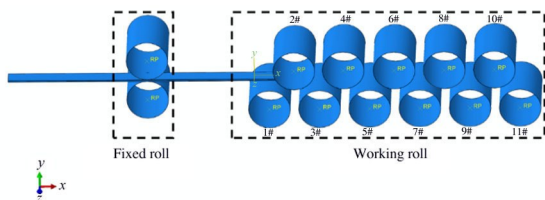


Fig.5 Schematic diagram of 11-roll straightening process model

Table 1 Basic parameters of straightener

Roll diameter/mm	Roll length/mm	Roll spacing/mm	Poisson's ratio	Velocity/rad·s ⁻¹	Static friction coefficient	Dynamic friction coefficient
95	2100	100	0.3	2	0.35	0.25

Table 2 Upper straightening roll reduction (mm)

Roll	2#	4#	6#	8#	10#
Reduction amount	0.724	0.465	0.290	0.155	0.000

Table 3 Basic parameters of clad layer and base layer materials

Layer	Material	Yield strength/MPa	Elastic modulus/GPa	Density/kg·m ⁻³	Poisson's ratio
Clad	S304	114	200	7.75	0.247
Base	Q235	127	210	7.85	0.300

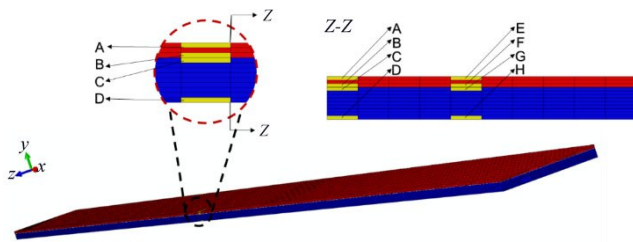


Fig.6 Schematic diagram of elements A~H in composite plate

the material, the equivalent plastic strain changes faster when the composite plate passes from the 4# roll to the 6# roll between 9.60~10.56 s. The equivalent plastic strain continues to increase, but the increment becomes smaller between 10.56~12.00 s. Due to the reduction effect of the 10# roll, the equivalent plastic strain barely changes when the composite plate passes from the 8# roll to the 10# roll between 12.00~13.44 s.

The equivalent plastic strain at element D is greater than that at element A, according to Fig.8a. The equivalent plastic

strain on both width-sides of composite plate is consistent with the equivalent plastic strain at the middle point, which agrees well with the variation law of equivalent force at the point with the same length and different widths. As shown in Fig.8, since the equivalent Mises stress of the bonding layer is lower than the yield strength, the equivalent plastic strain of elements F and G can be obtained when the thickness ratio of composite plate is 1:1. However, with increasing the equivalent plastic strain and decreasing the proportion of clad layer thickness, the gap between elements F and G is increased. Therefore, some hidden dangers may appear in the subsequent production and processing.

The stress nephograms of composite plates along y-axis at the 4# roll with different thickness ratios are shown in Fig.9. The touch point does not agree with the central axis of the straightener roll, and it is on the left side of the central axis. This result indicates that there is a contact angle between the composite plate and the straightener roll during the straightening process, and an obvious maximum stress region occurs at the central axis. As shown in Fig.9, the stress neutral layer is close to the clad layer.

In Fig.9a, it can be seen that the plastic deformation does not occur in the bonding layer. In Fig.9b and 9c, the obvious plastic strain occurs in the bonding layer. According to the stress nephogram, the step-like changes can be distinctly observed in the bonding layer. The stress neutral layer offsets of composite plate with the thickness ratio of 1:1, 1:3, and 1:5 are 0.1057, 0.1311, and 0.1442 mm, respectively. In addition, the maximum offset reaches 2.1% of the plate thickness. This result shows that the stress neutral layer offset plays an important role in the straightening of bimetal composite plates, which should be considered in the construction model and actual production. The residual stress of the composite

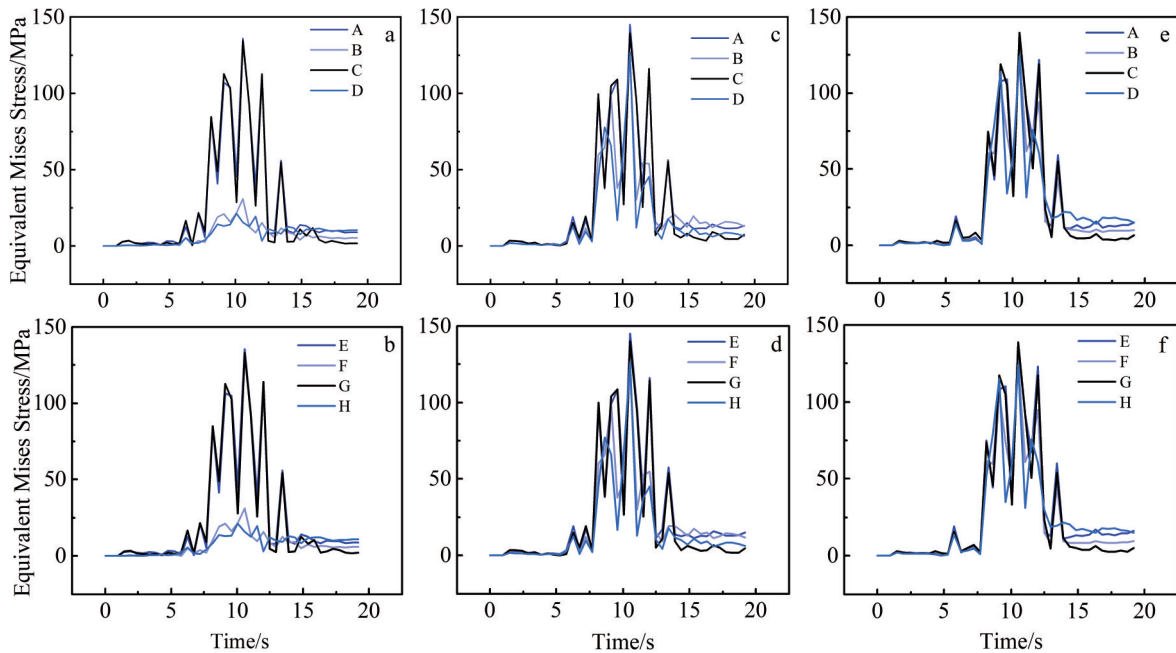


Fig.7 Equivalent Mises stress at elements A~D (a, c, e) and elements E~H (b, d, f) on bimetal composite plate with thickness ratio of 1:1 (a, b), 1:3 (c, d) and 1:5 (e, f)

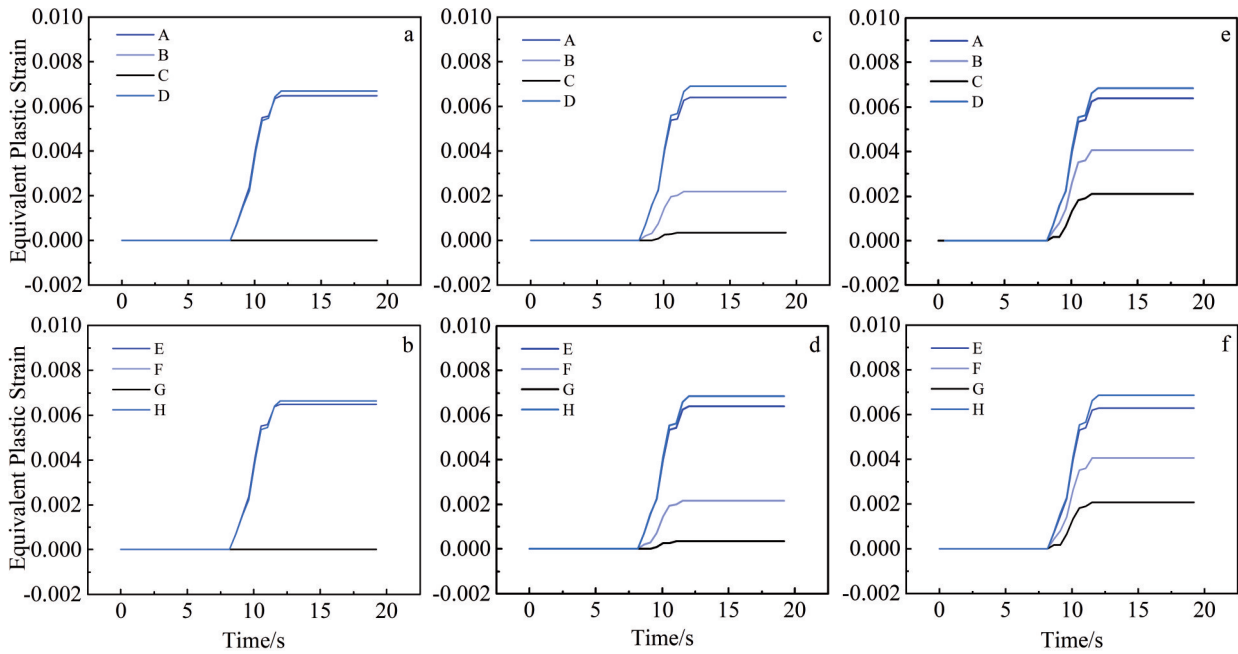


Fig.8 Equivalent plastic strains of elements A~D (a, c, e) and elements E~H (b, d, f) of bimetal composite plate with thickness ratio of 1:1 (a, b), 1:3 (c, d) and 1:5 (e, f)

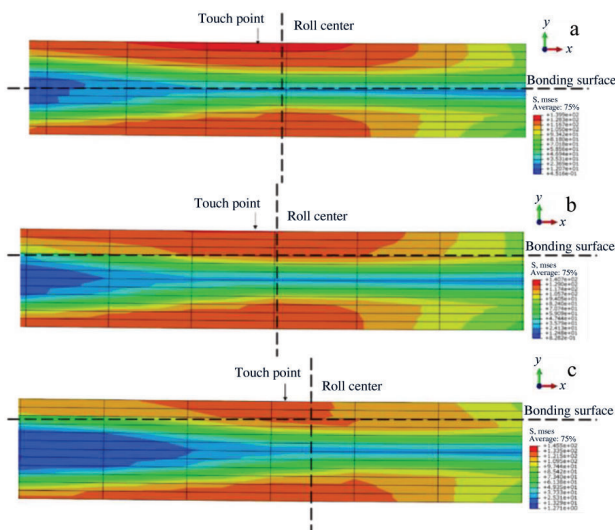


Fig.9 Stress nephograms of composite plates along y-axis at the 4# roll with thickness ratio of 1:1 (a), 1:3 (b), and 1:5 (c)

plates is small, and the clad layer exhibits a reverse yield phenomenon, which causes the springback of the composite plates and further breaking. Besides, the stress neutral layer offset of the composite plate under each roll can be calculated, as listed in Table 4.

According to Table 4, the absolute value of neutral layer

offset is increased firstly and then decreased with the strengthening process proceeding. The maximum neutral layer offset is achieved at the 4# roll, indicating that the composite plate is completely straightened due to the Bauschinger effect. Particularly, the Bauschinger effect causes the fact that the yield strength of the composite plate decreases during the continuous bending, compared with that at the 2# roll. With the strengthening process proceeding, the straightening force is decreased, resulting in a gradual decrease in the neutral layer offset. It can also be found that the displacement of the neutral layer offset is increased with increasing the proportion of base layer thickness, because the clad layer is entirely at the plastic deformation state when the thickness ratio of composite plate reaches 1:5, and the yield strength of the base layer is greater than that of the clad layer.

3 Experiment

The essence of the straightening process is the continuous bending deformation of the plate. The bending experiments were conducted to simulate the single straightening unit by the WDW-E100 multi-functional machine, as shown in Fig. 10. The material was S304/Q235 composite plate with the thickness ratio of S304 layer to Q235 layer of 1:1, 1:3, and 1:5. The plate length was 120 mm, the width was 50 mm, and the total thickness was 6 mm. Moreover, the force was 0.85, 1.27, and 1.33 kN under the thickness ratio condition of 1:1,

Table 4 Stress neutral layer offset of bimetal composite plates with different thickness ratios (mm)

Thickness ratio	2#	3#	4#	5#	6#	7#	8#	9#	10#
1:1	0.0638	-0.0711	0.1057	-0.1032	0.0976	-0.0828	0.0000	0.0000	0.0000
1:3	0.0702	-0.7851	0.1311	-0.1157	0.1007	-0.9142	0.0000	0.0000	0.0000
1:5	0.0864	-0.1041	0.1442	-0.1357	0.1124	-0.1024	0.0000	0.0000	0.0000

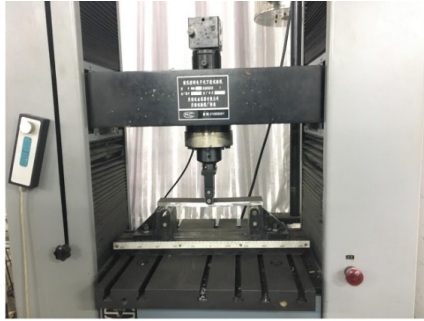


Fig.10 Bending experiment model

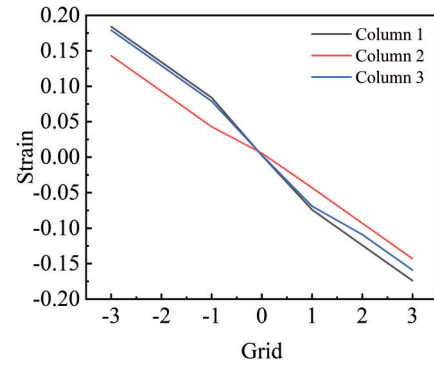


Fig.12 Strain distribution of S304/Q235 composite plate

1: 3, and 1: 5, respectively. The straightening force was obtained by the numerical simulations. The fulcrum distance was 95 mm. The composite plate was put inside a heating furnace, heated to 450 °C, and kept for 0.5 h. The cross-section of the bimetal composite plate was polished and meshed, as shown in Fig. 11. The deformed grid of the cross-section of composite plate was obtained, and the grid size was accurately measured by CAD software. The tensile deformation and compressive deformation of the composite plate were positive and negative, respectively. The experiment results are shown in Table 5. The strain distribution of the composite plate is shown in Fig.12.

As shown in Fig. 12, the longitudinal coordinate 0 is the position of the geometric center layer, and the horizontal coordinate 0 is the point where the pressure is applied by the indenter. Before the plate is deformed, the position of the strain neutral layer agrees well with the geometric center layer. The strain distribution of the three columns is basically linear along the thickness direction. The strain on the upper and lower surfaces is the highest, and the strain near the geometric center layer is relatively lower. The continuity of the shape deformation suggests that there is a fiber layer with zero strain, namely the neutral layer of the composite plate. As shown in Fig. 12, the strain neutral layer occurs on the loading

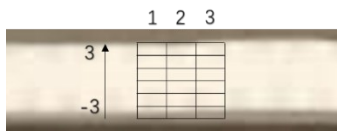


Fig.11 Cross-section and mesh grid of S304/Q235 composite plate

Table 5 Strain of S304/Q235 composite plate

Grid	1	2	3
3	-0.1740	-0.1430	-0.1590
2	-0.1240	-0.0930	-0.1090
1	-0.0740	-0.0430	-0.0690
0	0.0026	0.0057	0.0031
-1	0.0840	0.0430	0.0790
-2	0.1340	0.0930	0.1290
-3	0.1840	0.1430	0.1790

Table 6 Neutral layer offset of bimetal composite plates at the 4# roll by different methods (mm)

Thickness ratio	Theoretical calculation	Finite element simulation	Experiment
1:1	0.1102	0.1057	0.0820
1:3	0.1421	0.1331	0.1098
1:5	0.1608	0.1442	0.1325

side. The neutral layer offset in column 1, 2, and 3 is 0.022, 0.082, and 0.039 mm, respectively, which is obtained from the fitting calculation.

4 Results and Discussion

The neutral layer offsets of bimetal composite plates with different thickness ratios obtained by the theoretical calculations, finite element simulations, and experiments are presented in Table 6.

According to Table 6, it can be seen that the neutral layer offset is gradually increased with increasing the proportion of the base layer thickness, which is consistent with the influence factors of neutral layer offset calculated by the theoretical formula. This result also confirms the importance of the thickness ratio and yield strength of composite plate in the strengthening process, suggesting the accuracy of the theoretical calculation. Although the variation trend of neutral layer offset is basically the same under different methods, there are still some errors. In the theoretical deduction, the materials are considered as the ideal elastic-plastic materials; in the finite element analysis, some errors certainly exist in the algorithm of the analysis software and in the data fitting process. Therefore, even with the errors, the neutral layer offset of bimetal composite plates during the straightening process can be accurately obtained by the theoretical calculation.

5 Conclusions

1) The neutral layer offset is increased with increasing the proportion of base layer thickness in the composite plate. During the straightening process, the displacement of neutral

layer offset produced by the 4# roll is the longest.

2) With the strengthening process proceeding, the displacement of the neutral layer offset is gradually decreased.

3) The residual stress of S304 steel/Q235 aluminum composite plates is small, and the clad layer exhibits a reverse yield phenomenon, which causes the springback of the composite plates and further breaking.

References

- Li L, Yin F X, Tanaka Y et al. *Materials Transactions*[J], 2010, 51(5): 911
- Tian Yaqin, Qin Jianping, Li Xiaohong. *Development and Application of Materials*[J], 2006, 26(1): 40 (in Chinese)
- Ma Zhixin, Hu Jie, Li Defu et al. *Chinese Journal of Rare Metals* [J], 2003, 27(6): 799 (in Chinese)
- Xie Baochao, Guo Chenyang, Zhang Shiquan et al. *Journal of Constructional Steel Research*[J], 2020, 175: 106 326
- Chen WeiHua, Liu Juan, Cui Zhenshan et al. *Journal of Iron and Steel Research International*[J], 2015, 22(8): 664
- Dhib Z, Guermazi N, Ktari A et al. *Materials Science and Engineering A*[J], 2017, 696: 374
- Yazdani M, Toroghinejad M R, Hashemi S M. *Journal of Materials Engineering and Performance*[J], 2015, 24(10): 4032
- Belyaev S, Rubanik V, Resnina N et al. *Physics Procedia*[J], 2010, 10: 52
- Kang G T, Song J S, Hong S I. *Advanced Materials Research*[J], 2014, 951: 83
- Jia W T, Ma L F, Le Q C et al. *Journal of Alloys and Compounds* [J], 2019, 783: 863
- Mehrara M, Nategh M J. *Proceedings of the Institution of Mechanical Engineers: Part B*[J], 2011, 226(4): 722
- Arikök R, Mecitoglu Z. *2010 International Mechanical Engineering Congress and Exposition*[C]. Vancouver: ASME, 2010, 9: 321
- Sun Zhihui, Chen Wenyuan. *Applied Mechanics and Materials* [J], 2013, 239-240: 680
- Knight C W, Hardy S J, Lees A W et al. *Ironmaking & Steelmaking*[J], 2002, 29(1): 70
- Morris J W, Hardy S J, Thomas J T. *Ironmaking & Steelmaking* [J], 2005, 32(5): 443
- Huh H, Lee H W, Park S R et al. *Journal of Materials Processing Technology*[J], 2001, 113(1-3): 714
- Kano H, Kenmochi K. *Kawasaki Steel Giho (Japan)*[J], 2001, 33(3): 112
- Cui Li, Shi Quanqiang, Liu Xianghua et al. *Journal of Iron and Steel Research International*[J], 2013, 20(10): 23
- Guan Ben, Zhang Chao, Zang Yong et al. *Chinese Journal of Mechanical Engineering*[J], 2019, 32: 47
- Zhang Chao, Zang Yong, Guan Ben et al. *Journal of Zhejiang University (Engineering Science)* [J], 2017, 51(8): 1575 (in Chinese)
- Dharani L R, Chai L, Pagano N J. *Composites Science and Technology*[J], 1990, 39(1): 29
- Wang Lifei, Huang Guangsheng, Pan Fusheng et al. *Materials Letters*[J], 2015, 143: 44
- Huang Guangsheng, Wang Yanxia, Wang Lifei et al. *Transactions of Nonferrous Metals Society of China*[J], 2015, 25(3): 732
- Ma Lifeng, Ma Ziyong, Jia Weitao et al. *The International Journal of Advanced Manufacturing Technology*[J], 2015, 79(9-12): 1519
- Zuo Duquan, Cao Zengqiang, Cao Yuejie et al. *Proceedings of the Institution of Mechanical Engineers Part C: Journal of Mechanical Engineering Science*[J], 2020, 234(14): 2881
- Zhao Mingji, Huang Kepeng, Wang Fazhan. *Coal Mine Machinery*[J], 2020, 41(2): 92 (in Chinese)
- Gui Hailian, Xing Tong, Li Yugui et al. *Materials Research Express*[J], 2019, 6(8): 86 569
- Gui Hailian, Ma Lifeng, Wang Xiaogang et al. *Applied Mathematical Modelling*[J], 2017, 50: 732
- Gui Hailian, Li Yao, Song Hao et al. *Advances in Materials Science and Engineering*[J], 2015, 2015: 863 610
- Gui Hailian, Li Qiang, Li Yao et al. *Journal of Marine Science and Technology*[J], 2014, 22(5): 3
- Wang Yadong, Liu Cuirong, Ma Lifeng et al. *Rare Metal Materials and Engineering*[J], 2021, 50(12): 4395 (in Chinese)
- Song Hao. *Thesis for Master*[D]. Taiyuan: Taiyuan University of Science and Technology, 2017 (in Chinese)

不同厚度比 S304/Q235 复合板矫直过程中性层的偏移规律

邢 彤^{1,2}, 刘翠荣³, 马立峰¹, 李 强⁴, 李玉贵², 楚志兵^{1,3}, 王效岗¹, 桂海莲^{1,3}

(1. 太原科技大学 重型机械教育部工程研究中心, 山西 太原 030024)

(2. 太原科技大学 机械工程学院, 山西 太原 030024)

(3. 太原科技大学 材料科学与工程学院, 山西 太原 030024)

(4. 太原重型机械集团 技术中心, 山西 太原 030024)

摘要: 为了提高 S304/Q235 复合材料矫直过程的精度, 在 Abaqus 有限元软件中分析了双金属复合材料板的弹塑性变形和矫直过程。此外, 对不同厚度比双金属复合板的中性层偏移进行了分析研究。结果表明, 双金属复合板的中性层偏移量取决于复合板的屈服强度和厚度比。将理论计算、数值模拟和实验结果进行对比, 得到了中性层偏移量的拟合公式, 验证了其正确性, 分析了中性层偏移状态的动态变化。本研究为建立高精度矫直力模型提供了理论依据。

关键词: 厚度比; 中性层偏移; 双金属复合板; 矫直

作者简介: 邢 彤, 男, 1989 年生, 博士生, 太原科技大学重型机械教育部工程研究中心, 山西 太原 030024, E-mail: 120025062@qq.com